PERIODICA POLYTECHNICA SER. TRANSP. ENG. VOL. 31, NO. 1–2, PP. 53–78 (2003)

COMPUTATIONAL INVESTIGATION ON DESWIRL VANES FOR MULTISTAGE CENTRIFUGAL COMPRESSORS

Árpád VERESS

Department of Aircraft and Ships
Budapest University of Technology and Economics
H–1111 Budapest, Sztoczek u. 6, J ép. 4.em. 426, Hungary
Tel: (36) 1-463-1992
e-mail: veress@rht.bme.hu

Received: Aug. 31, 2002

Abstract

The goal of this project is to report on some computational investigations about the return flow passages. The return flow channel provides the connection and carries the flow between two stages of a multistage centrifugal compressor. Of course, deswirl vanes are indispensable between the inlet and outlet section, because usually the inlet flow angle, which comes from the impeller, is $70° - 75°$ measured from radius and the downstream flow angle should be axial, for the next stage. Generally, the shape of this unconventional blade is unique; it is not possible to choose it from any catalogues.

During the design procedures, a couple of new blade design techniques have been developed; among them one is based on a zero circulation over the control surface, between two blades with the meaning of CBL (constant blade loading) [14]. The purpose of this investigation is to construct a 3D blade for the return passage. In addition, a system of programs for UNIX was developed to help us to communicate between the different software. The next step is to use the inviscid inverse design program to make the most relevant blade; provided by the CBL design, as perfect as possible and introduce negative and positive lean to improve the design specifications. Finally, we should analyse the configuration with a 3D Navier-Stokes solver to have some conclusions about the new blade geometry.

Of course, in the design process, the loss coefficient and pressure recovery factor are the two main parameters, which are always taken into consideration to check the correctness of the design.

Keywords: return flow channel, inverse design method, Euler and Navier-Stokes solver.

1. Introduction

In most multi-stage centrifugal compressors a big amount of the energy, imported to the fluid leaving the impeller of a given stage, is in the form of kinetic energy or velocity with meridional and tangential components. To ensure a good efficiency and further pressure recovery it is necessary to convert as much kinetic energy as possible into static pressure before the fluid is entering the next stage. The objective of a return channel is furthermore to change the flow direction from the radial-tangential direction to an axial direction.

In general, a return channel of a conventional radial multi-stage compressor consists of all or some of the following components:

- A vaneless or vaned diffuser, which partially diffuses the flow leaving the impeller.
- An annular passage, which directs the flow from the exit of the vaneless diffuser to the inlet of the next stage.
- And finally a set of vanes somewhere after the bend section to remove the swirl in the flow and to recover some of the kinetic energy in the remaining velocity after passing the diffuser and the bend.

In order to optimise the whole crossover system, there appears very little that can be done to change the efficiency and pressure recovery of the vaneless diffuser. Big losses occur in the crossover system where the flow undergoes a strong turning. THYGESEN in his work showed, that better efficiency is possible if deswirl vanes extend over the return bend [10].

The vane geometry can be varied in many ways and there is also a free choice of the location of trailing edge and leading edge and number of the vanes. The objective of this report is to make use of these opportunities, which are left over in the design process of return channel blades. Thus, improvements in the design of the vanes should be possible, and furthermore, if the efficiency and pressure recovery factor of the vanes can be improved, less diffusion in the vaneless diffuser may be required, which can materially reduce the overall compressor size.

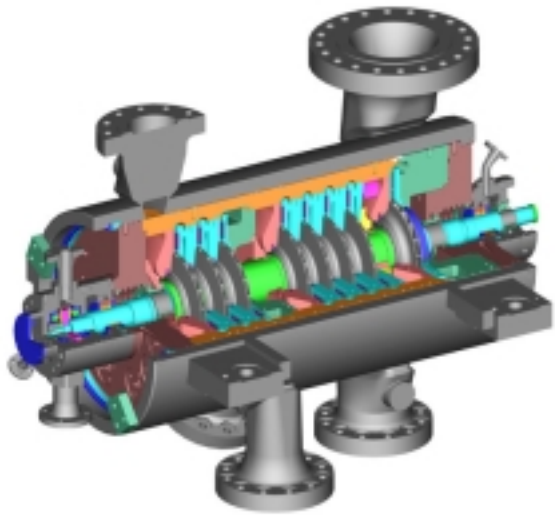

Fig. 1. Dresser-Rand DATUM multi-stage centrifugal compressor

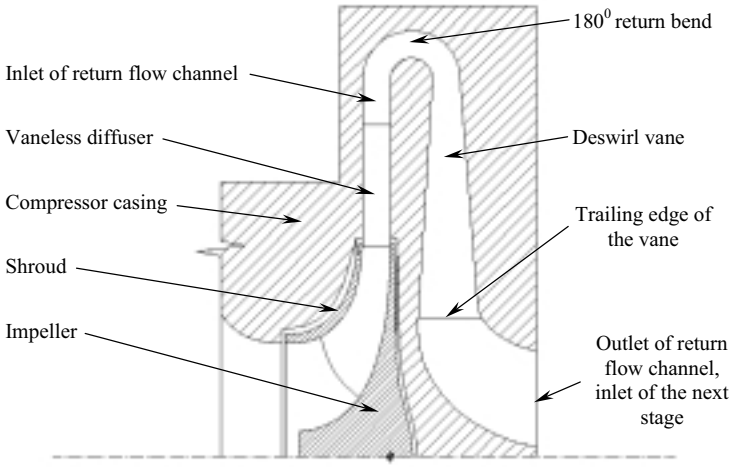

Fig. 2. Meridional cross section about the configuration

2. Design Parameters

The next two parameters should always be checked for every crossover configuration to guide the design.

Loss coefficient: $\omega = \dfrac{\overline{p}^{\text{to}}_{\text{in}} - \overline{p}^{\text{to}}_{\text{out}}}{\overline{p}^{\text{to}}_{\text{in}} - \overline{p}^{\text{st}}_{\text{in}}}$; which indicates what part of the available kinetic energy is dissipated by the pressure losses, with $\overline{p}^{\text{to}}_{\text{in}} = \overline{p}^{\text{st}}_{\text{in}} + \overline{p}^{\text{dyn}}_{\text{in}}$; and $\overline{p}^{\text{to}}_{\text{out}} = \overline{p}^{\text{st}}_{\text{out}} + \overline{p}^{\text{dyn}}_{\text{out}}$.

Pressure recovery factor: $C_p = \dfrac{\overline{p}^{\text{st}}_{\text{out}} - \overline{p}^{\text{st}}_{\text{in}}}{\overline{p}^{\text{to}}_{\text{in}} - \overline{p}^{\text{st}}_{\text{in}}}$; which quantifies what part of the kinetic energy has been converted into static pressure. This coefficient is also important, because along the diffuser and return passage we would like to reach as much pressure rise as possible.

3. Computational Tools

3.1. Euler Solver

The basis of the inverse design code is an Euler solver. The solver is a cell-centered finite volume method that solves the time dependent Euler equations that are presented next:

$$\frac{\partial}{\partial t}\iiint U \,\mathrm{d}v + \iint Hn \,\mathrm{d}A = 0;$$

in which:

$$U = \begin{pmatrix} \rho \\ \rho W_r \\ \rho W_\theta \\ \rho W_z \\ \rho e \end{pmatrix}$$

and

$$H = \begin{pmatrix} \rho W_r + \rho W_\theta + \rho W_z \\ \left(\rho W_r^2 + p\right) + \rho W_r W_\theta + \rho W_r W_z \\ \rho W_r W_\theta + (\rho W_\theta^2 + p)_{i\theta} + \rho W_\theta W_z \\ \rho W_r W_z + \rho W_\theta W_z + \rho (W_z + p)_{iz} \\ \rho W_r (e + \frac{p}{\rho}) + \rho W_\theta (e + \frac{p}{\rho}) + \rho W_z (e + \frac{p}{\rho}) \end{pmatrix}.$$

The method implements the following features: flux vector splitting, MUSCL differencing, limiters, Runge–Kutta time integration and convergence acceleration techniques such as local time stepping, rothalpy damping and residual averaging.

These techniques are fully described in references [3] and [4].

3.2. Inverse Design Program

The program is based on a 3D Euler solver developed by DEMEULENAERE. A full description can be found in [3] and [4]. The 3D inverse code is an extension of the 2D inverse program of LEONARD [5]. The basic principle of the inverse design is to start from an initial geometry for which the corresponding velocity distribution is obtained. In the second step a pressure or velocity distribution (target distribution) is imposed as shown in *Fig. 3*. In most cases the target distribution is imposed at the hub and tip section, but it is up to the designer to choose in how many sections he wants to specify the Mach number distribution along the span of the blade. The final imposed distribution over the span of the blade is obtained by interpolation between the given sections.

3.3. Navier–Stokes Solver – TASCflow3D (CFX)

Using 3D NS solver, information has been provided about loss coefficient and pressure gain. The Program Turbogrid generates a 3-dimensional structured computational grid, on which the governing viscous equations are solved. The grid must be supplied in terms of the x, y and z locations of the grid nodes distributed throughout the computational domain. The flow code uses a cell centered control volume approach. At each node in the domain, the flow code will determine values for all dependent variables such as pressure, velocity components, temperature, turbulence quantities, etc.

There are two capabilities of the grid generator that expand the flexibility of the structured grid constraint. First, grid-embedding provides the ability to locally

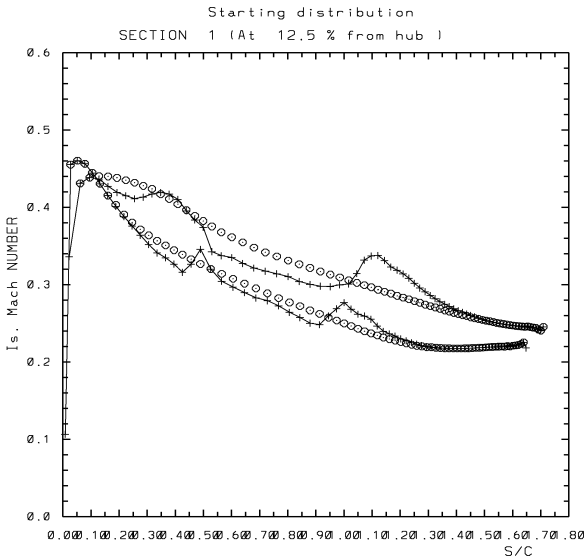

Fig. 3. Original (+) and imposed (o) velocity distributions

refine a coarse structured grid with a finer structured grid. Secondly, grid-attaching makes it possible to merge two dissimilar structured grids.

The flow code TASCflow3D uses an implicit scheme to solve the discretized equations and the $k - \varepsilon$ turbulence model with wall model as a boundary layer model.

4. Inverse Design of Deswirl Vane

In order to be able to define the initial blade geometry for the inverse design program, it seemed to be the best solution to develop a reproducible multi-parameterised blade design program. The input of the BLADECONTOUR code is as follows: blade angle distribution, thickness distribution and the co-ordinates of meridional cut of the return flow channel. The output of the program is as follows: co-ordinates of the hub and shroud section of the blade with appropriate camber lines for inviscid: cylindrical (m, Rtheta, R) and for viscous calculation: Cartesian (x, y, z) space. During the computation one can modify the location of the trailing edge and leading edge and the location of maximum thickness. The most relevant blade angle distribution is called CBL (Constant Blade Loading) blade design. The full description and features of this method with the BLADECONTOUR program can be found in [14].

The meridional cross section of the configuration and the blade profiles at hub, middle and shroud with viewing from axis direction are demonstrated in *Fig.4*. This

geometry is used for the inviscid computation and the results of the Euler solver are shown in *Fig. 5*.

Two critical parts can be seen in the Mach number distribution of *Fig.5*. One of them is upstream and another one is downstream of the crossover bend. When the return bend starts, the radial velocity increases at the hub and decreases at the shroud section because of convex and concave curvature effect. The result of this phenomenon is a decrease of the blade loading at the hub section (the flow turns itself to more radial) and an increase of the blade loading at the shroud (the flow turns against the blade towards more tangential). Downstream of the bend the curvature effect is eliminated and flow becomes uniform, which results a decceleration at the hub and acceleration at the shroud section in the radial direction. The flow tries to turn against the blade – more loading – at the hub and tries to turn with the blade – less loading – at the shroud section. These sudden peaks in the Mach number distribution are responsible for the huge separation bubble at the suction side of the blades, which were always visible in the results of the N-S solver (*Fig. A1*). In this case, the goal of inverse design is to reduce the negative effects of the channel meridional curvature by imposing smoother Mach number distributions than in *Fig. 5*.

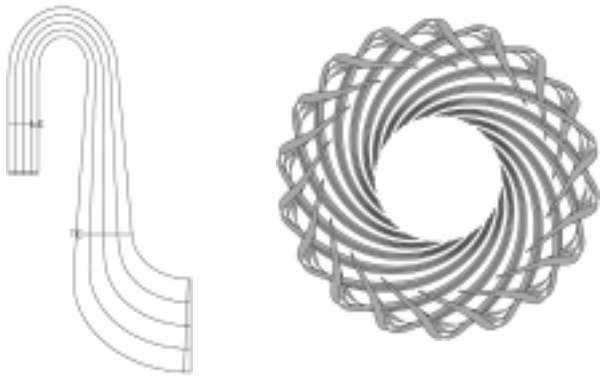

Fig. 4. Return passage meridional cross section (on the left side) and hub, middle and shround section of the blades in the R-Theta plane for constant blade loading

The next step is to use the inverse design program to make the blade contour as suitable as possible for a given flow field. The inverse solver was fully converging, and results can be found in *Fig. 6* after 550 iterations.

It is also very interesting to make a comparison between the original and inverse redesigned blade contour in *Fig. 7*. This blade geometry has been used for lean angle investigation.

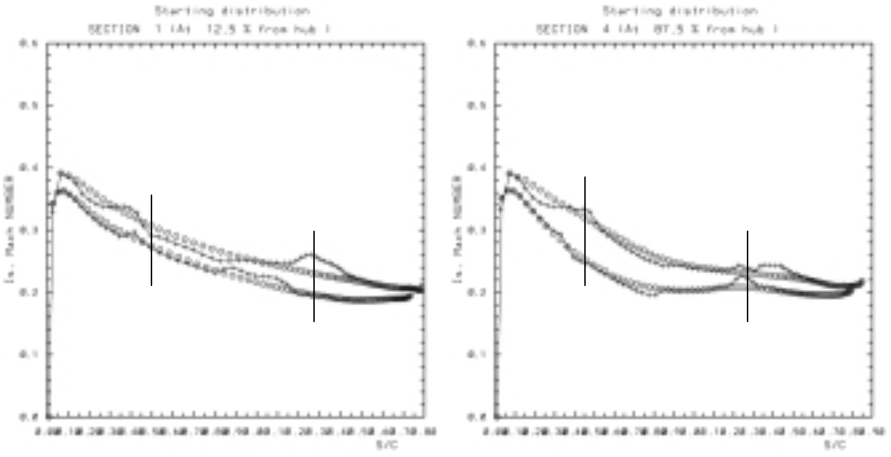

Fig. 5. Original (results of Euler solver) (+) and imposed (o), hub (on the left side) and shroud Mach number distribution

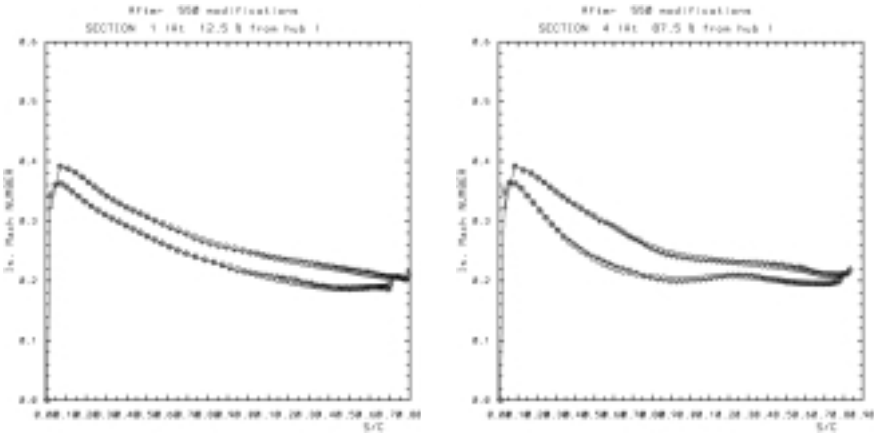

Fig. 6. Actual (results of inverse design) (+) and imposed (o), hub (on the left side) and shroud Mach number distribution

5. Lean Angle Effect

In the return flow channel there are two main effects defining the secondary flow:

- One of them is the passage vortex (PV) due to the flow turning forced by the blades. The velocity of the flow decreases inside the boundary layer at both

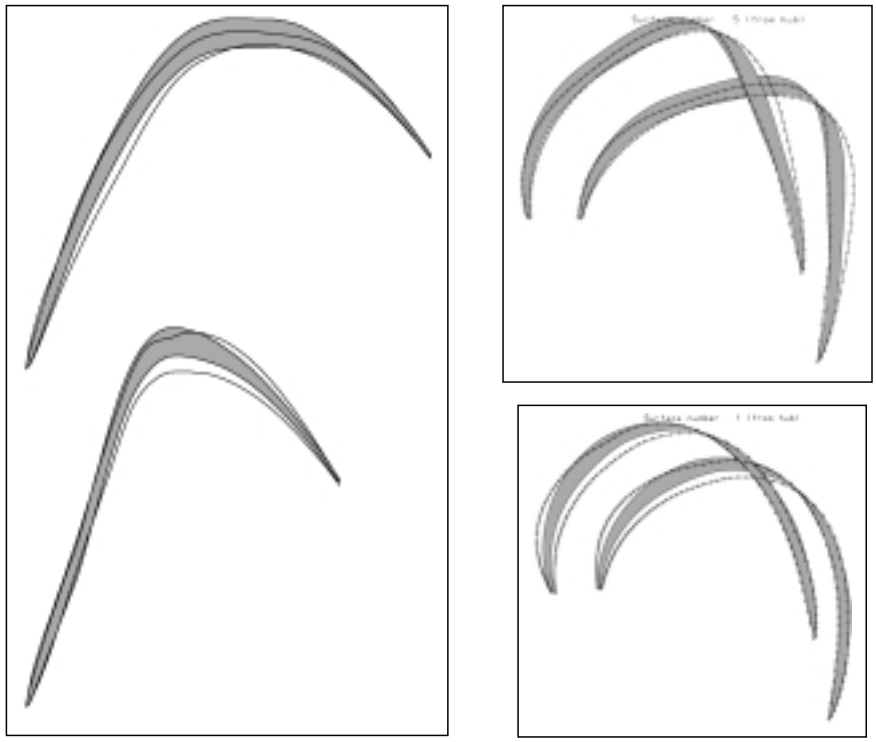

Fig. 7. Original (with grey shaded) and inverse designed hub (below) and shroud profiles (on the left side is in *m*-Rtheta plane with one blade and the other side is R-Theta plane with two blades)

the hub and shroud section. Because of constant pressure gradient between the pressure and suction side, the curvature of the streamline should increase (curvature radius should decrease), as it is shown in *Fig. 8.* The passage vortex starts from the leading edge, because the hub and shroud boundary layer exists and finishes at the trailing edge, because the suction side and pressure side pressure gradient has disappeared.

- The other phenomenon, which is causing also secondary flows, is the Blade surface Vortices (BV) generated by the meridional curvature of the channel. It will develop in the 180° crossover bend and in the radial-to-axial elbow at the outlet of the return flow channel. In this case the development of secondary flow is very similar to the passage vortex, but the deviation effect is due to the convex-concave curvature of the meridional contour, generating shroud to hub pressure differences, instead of pressure side – suction side pressure differences (*Fig. 8*).

The boundary layer is thicker in the outlet elbow than in the return bend, so the flow is more sensitive for BV (*Fig. A8*). The main idea of this part is to reduce the BV secondary flow using blade lean between the hub and shroud section. When introducing lean, the pressure distribution is going to be changed according to *Fig. 10*. The evaluated pressure distribution acts against the secondary flow, so it has a good effect to dump the BV (*Fig. A9*).

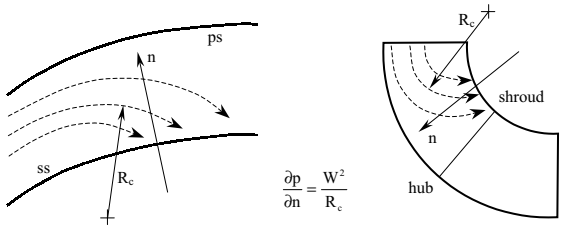

Fig. 8. Passage (on the left side) and blade vortices developments

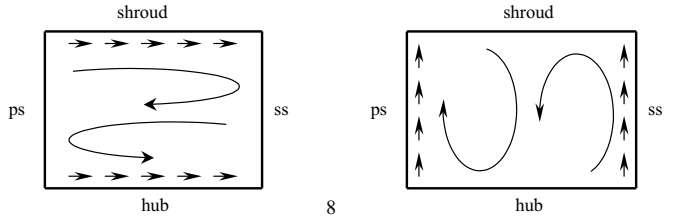

Fig. 9. Passage (on the left side) and blade vortices

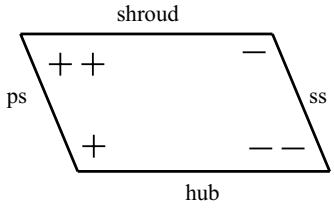

Fig. 10. Pressure distribution deviation by lean

The viscous calculation, concerning the lean angle effect has been performed for the design condition of CBL (Constant Blade Loading) with inverse designed blade.

The lean introduced in the design is shown in *Figs.12* and *13* where the original blade is compared with the new blade situation and also the channel geometry (*Fig. 11*) with the location of the blade is shown.

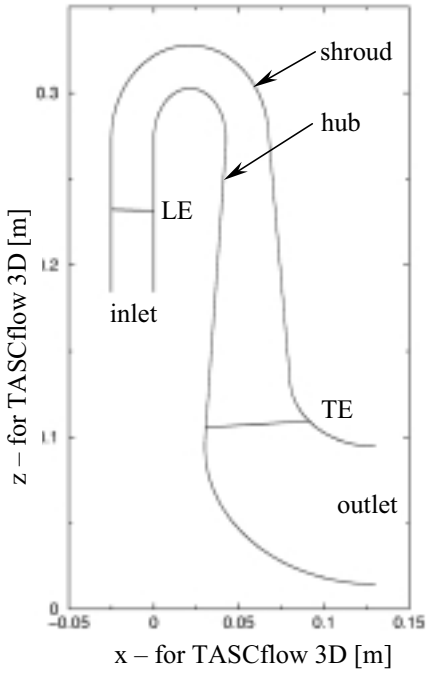

Fig. 11. Channel geometry with included blade

All dimensions are in meter. The lean angle has been realised by rotating all points of the shroud blade section around the machine axis with 4° into the direction of suction side resulting in a negative lean. It means about 27° maximum lean at the middle part of the crossover bend. The results of CFX for comparison can be found in *Figs. A8 – A10* in the case of no, negative and positive lean.

6. Results, Conclusions and Future Plan

6.1. Results

A couple of another blade design procedures have been developed for comparison. In these cases no inverse design and no lean angle were applied. Thus viscous calculation has been made for NON-EXTENDED (means that the blade starts only at the return passage without crossing the return bend) (*Fig. A1*), ACAD (3D blade design by 2D drawing in AutoCad) (*Figs. 14* and *A2*), LBAD (Linear Blade Angle Distribution, which means that β_{bl} is changing linearly along the vane (*Fig. 15*) and in the crossover bend one tries to keep the same blade angle, because this part of the channel is the most crucial for separation) (*Fig. A3*) and CBL (Constant Blade

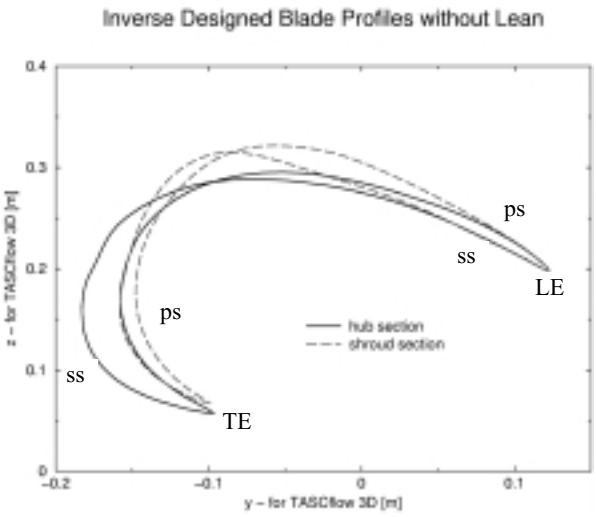

Fig. 12. Original blade situation

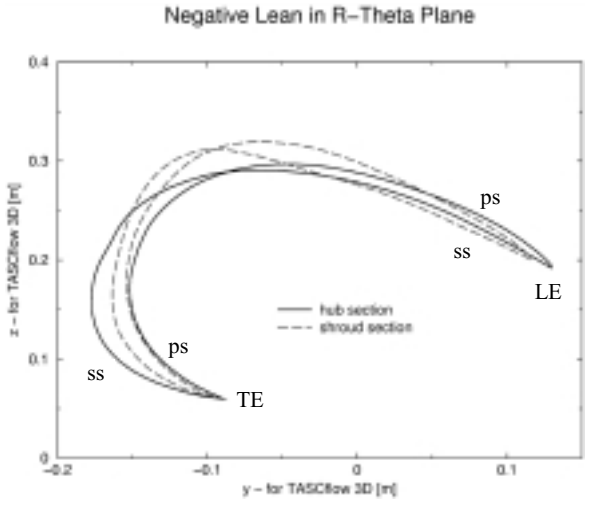

Fig. 13. Lean angle visualisation

Loading [14]) (*Fig. A4*) blade designs to allow some comparison between these and the CBL with inverse designed (*Figs. A5* and *A6*) and lean introduced blade design. The input data of the calculation come from the 100% rotor RPM [14].

The main characteristic of the NON-EXTENDED, ACAD, LBAD and CBL designs is a huge separation bubble on the suction side caused by the suddenly decreasing velocity. At the NON-EXTENDED design the length of the vane is too

short. The flow deviation by the blade from the tangential to axial has been realised along such a short distance that the flow most probably will separate (*Fig. A1*). On the other hand, the incidence angle is not appropriate either. The ACAD design has also problems with the non-optimum incidence resulting other return flow (separation bubble) occurring at the suction side of the blade at the return passage (*Fig. A2*). Principally, the first part of the LBAD designed blade is suffering from the sudden changes of velocity, so it is separated also (*Fig. A3*). If we use the CBL design without inverse redesign, the separation bubble also develops at the suction side of the blade in the return passage (*Fig. A4*). But in the case of CBL with inverse redesigned blade design the separation bubble has been completely eliminated (*Figs. A5* and *A6*).

The most important characteristic for the comparison is the loss coefficient and pressure recovery factor, which together with other parameters (using approximate face mass flows for averaging) can be found in the *Table 1*.

The results show that the best design is the inverse designed blade with CBL and negative lean. It has the smallest loss coefficient and the highest pressure recovery factor. The constant blade loading redesign by the inverse computation is the most powerful in such a complicated geometry as a return flow channel.

The negative lean, according to theory, which was mentioned in chapter 5, also improves the flow features (*Figs. A8–A9* for comparison).

Finally, we can take a comparison between the NON-EXTENDED and CBL with inverse redesign blade design cases about the flow field for 80% rotor RPM [14]. We can conclude for an off-design point also that the separation bubble also exists in the case of NON-EXTENDED blade design, but for the best design it has been completely eliminated.

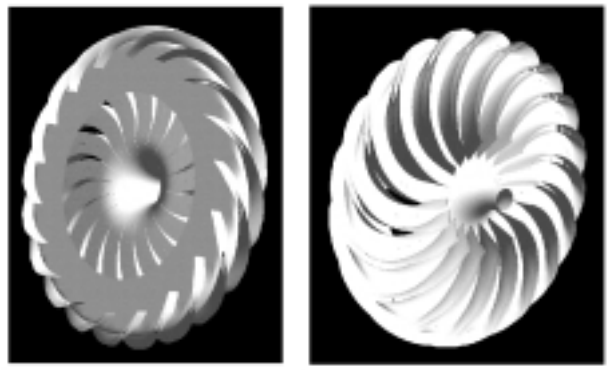

Fig. 14. Forward (on the left side) and backside view of the return flow channel with removed shroud casing by ACAD design

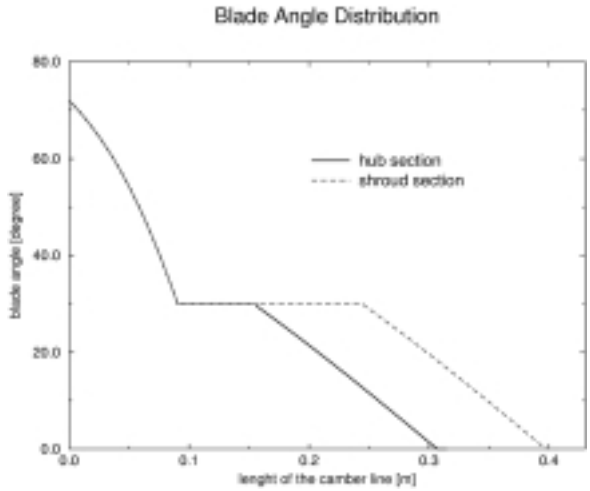

Fig. 15. Beta distribution for (LBAD) linear blade angle distribution

Table 1. Results of different configurations

Design	NON-EXTENDED	ACAD	LBAD	CBL
$p_{\text{in}}^{\text{to}}$ [Pa]	299699.1	299708.7	299701.8	299526.6
p_{in} [Pa]	159038.5	177780.9	174660.4	182298.2
$p_{\text{out}}^{\text{to}}$ [Pa]	236665.3	231072.9	231455.5	261108.8
p_{out} [Pa]	225215.1	224682.9	224379.6	258238.5
ω	**0.44813**	**0.5629**	**0.5458**	**0.3277**
$\mathbf{C}_p$	**0.4705**	**0.3847**	**0.3976**	**0.6478**
Mass flow [kg/s]	4.68	4.59	4.68	4.5

Design	CBL+ INVERSE	CBL + INVERSE+ NEGATIVE LEAN	CBL + INVERSE+ POSITIVE LEAN
$p_{\text{in}}^{\text{to}}$ [Pa]	299696.6	299698.5	299700.9
p_{in} [Pa]	174936.4	169050.8	186212.6
$p_{\text{out}}^{\text{to}}$ [Pa]	264954.2	265275.3	267900.2
p_{out} [Pa]	258414.2	258119.0	258616.7
ω	**0.27847**	**0.26348**	**0.280211**
$\mathbf{C}_p$	**0.669106**	**0.68174**	**0.63799**
Mass flow [kg/s]	4.5	4.5	4.5

6.2. Conclusions

The problem in THYGESEN's investigation, and at the beginning in this project also, was that the inverse code was not converging. To obtain the imposed velocity in a meridional contour with an extreme change of curvature radius at the crossover bend, seemed to be an insolvable task, without any negative thickness or increasing residuals, for the inverse design calculation. According to our experience the inverse design program can be made always convergent for any kind of strange geometry, if the difference between the initial and inverse redesign blade profile shape and area is less than 10–20%, depending on the difficulties of the meridional geometry.

On the other hand, the results of the N-S solver show a perfect evolution from the first design to the latest one concerning the design parameters; the loss coefficient and pressure recovery factor. We can conclude that the extension of the blade over the 180° crossover bend is an interesting idea to reduce the losses and increase the pressure recovery factor. If the losses are decreased it is possible to reduce the size of the geometry, which means saving with the expensive casing.

Finally, also the introduced negative lean improves the design parameters.

6.3. Future Plan

Using the experience of this project, it seems to be an interesting idea to take some computational investigations about the effects of radial length, curvature of the return bend and diffusivity change on return passage geometry, concerning the overall loss coefficient and pressure recovery factor.

A different radial length and shape of the return passage can produce different magnitudes of losses. It is a challenging task to find the way to reduce the radial length of the channel, as an optimisation procedure using an inverse design, an artificial neural network or other optimisation procedures to take some investigations about viscous flow without increasing the losses all over the channel.

List of Symbols and Abbreviations

a	: speed of sound
c	: chord
C_p	: pressure recovery factor
$\mathrm{d}n$, Δn	: normal elementary distance
$\mathrm{d}v$	: elementary volume
$\mathrm{d}A$	: elementary surface
$\mathrm{d}s$	: elementary displacement
$\mathrm{d}t$, Δt	: tangential elementary distance
T	: temperature
e	: specific internal energy
H	: flux vector of flow field
i	: spatial nodes
$\overline{m}$	: meridional vector
$\dot{m}$	: mass flow
n	: (outward) normal direction
U	: vector conservative variable
p	: pressure
r	: radial direction and distance
R_c	: curvature radius
t	: time
x, y, z	: Cartesian co-ordinate system
W	: relative velocity
z	: axial distance
	: static (for pressure)
*	: approximated value
bl	: blade
dyn	: dynamic (for pressure)
in	: inlet
is.	: isentropic
LE	: leading edge
n	: normal component
n	: time lever
ps	: pressure side
RPM	: revolution per minute
ss	: suction side
st	: static
t	: tangential component
T	: trailing edge
to	: total
out	: outlet
$\bar{}$	: average value

α : absolute flow angle
β : relative flow and blade angle
δ_{th} : blade thickness
ρ : density
θ : angular displacement
ω : loss coefficient

Appendix
Results of Navier-Stokes Solver

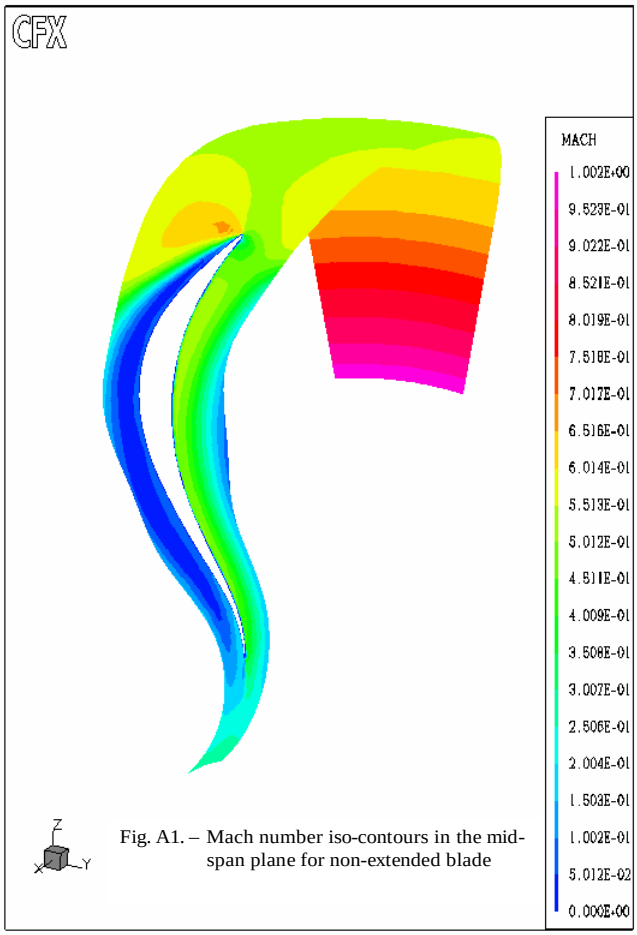

Fig. A1. – Mach number iso-contours in the mid-span plane for non-extended blade

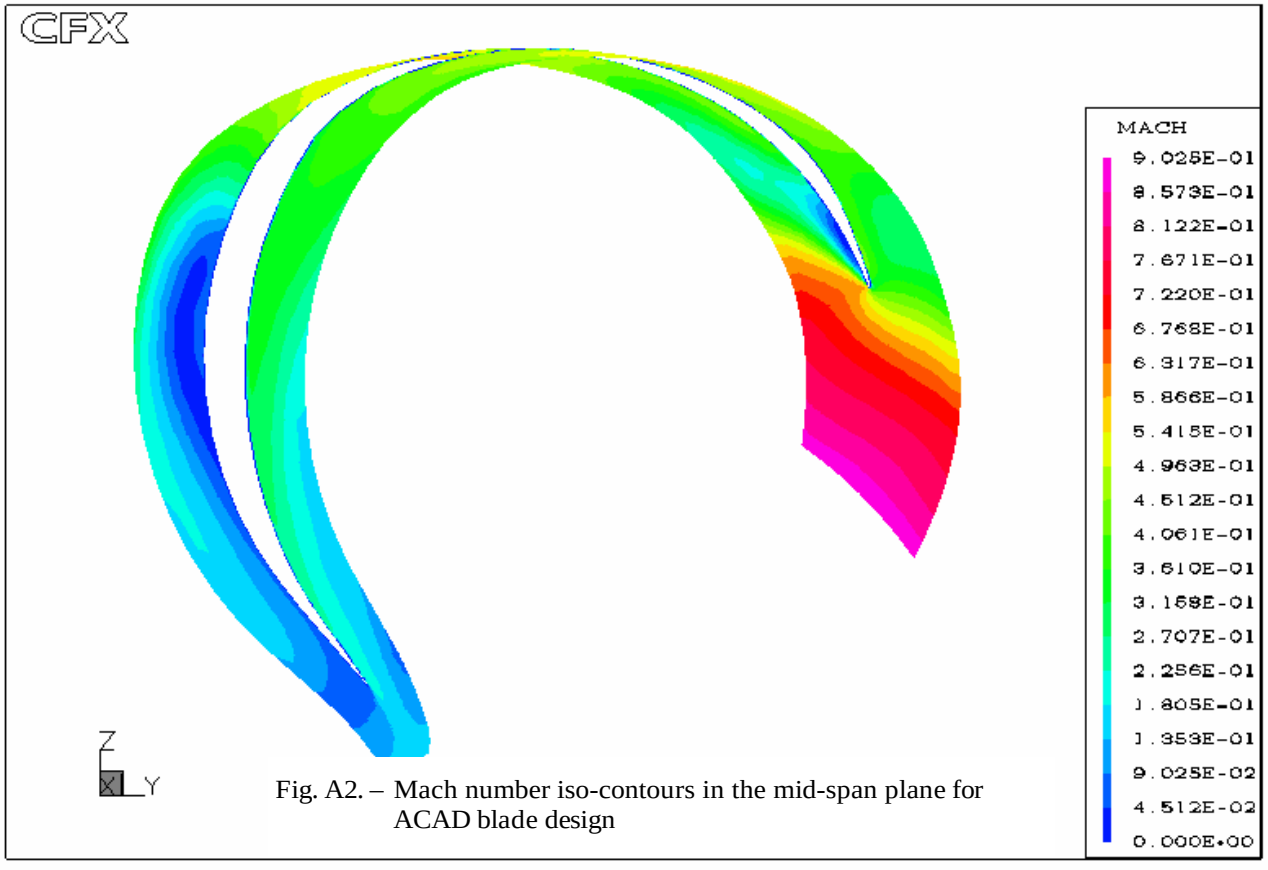

Fig. A2. – Mach number iso-contours in the mid-span plane for ACAD blade design

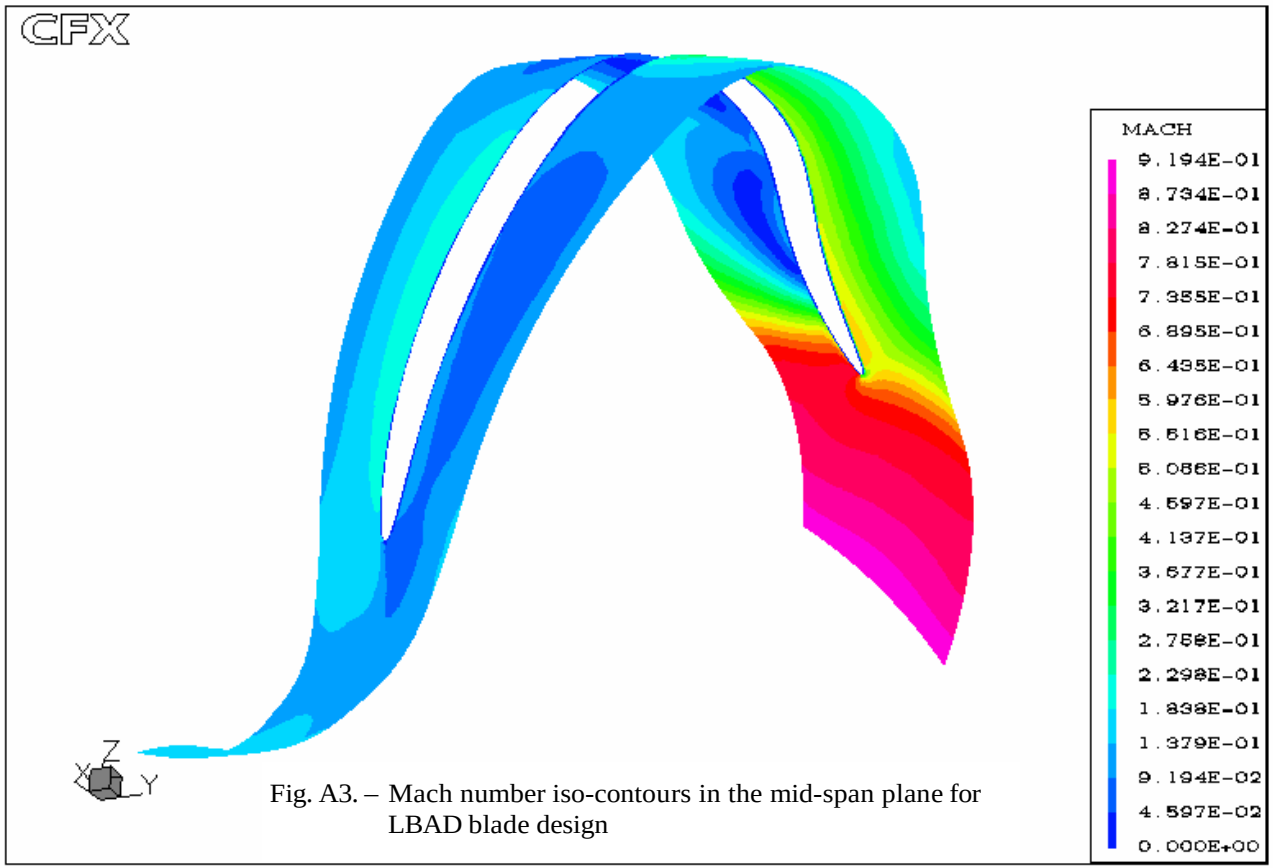

Fig. A3. – Mach number iso-contours in the mid-span plane for LBAD blade design

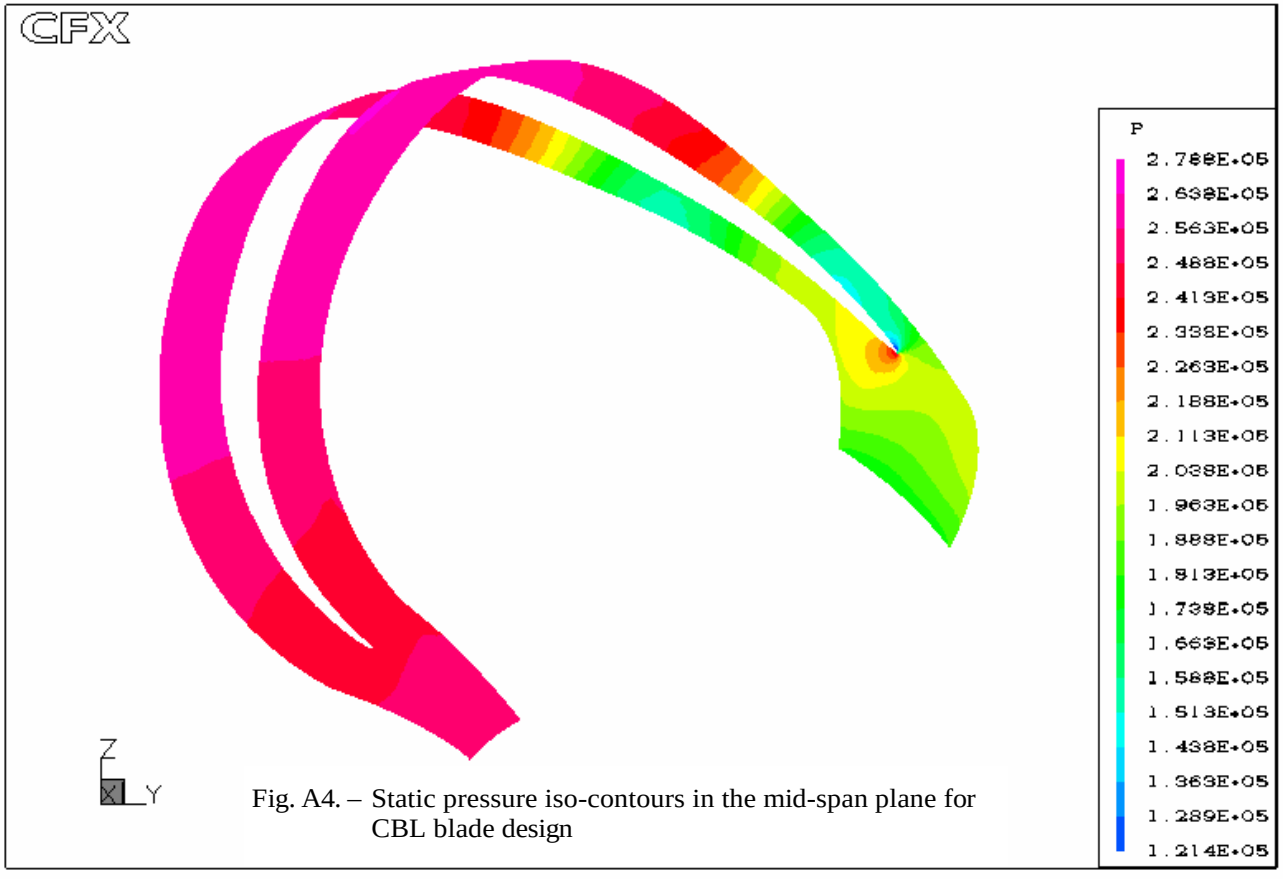

Fig. A4. – Static pressure iso-contours in the mid-span plane for CBL blade design

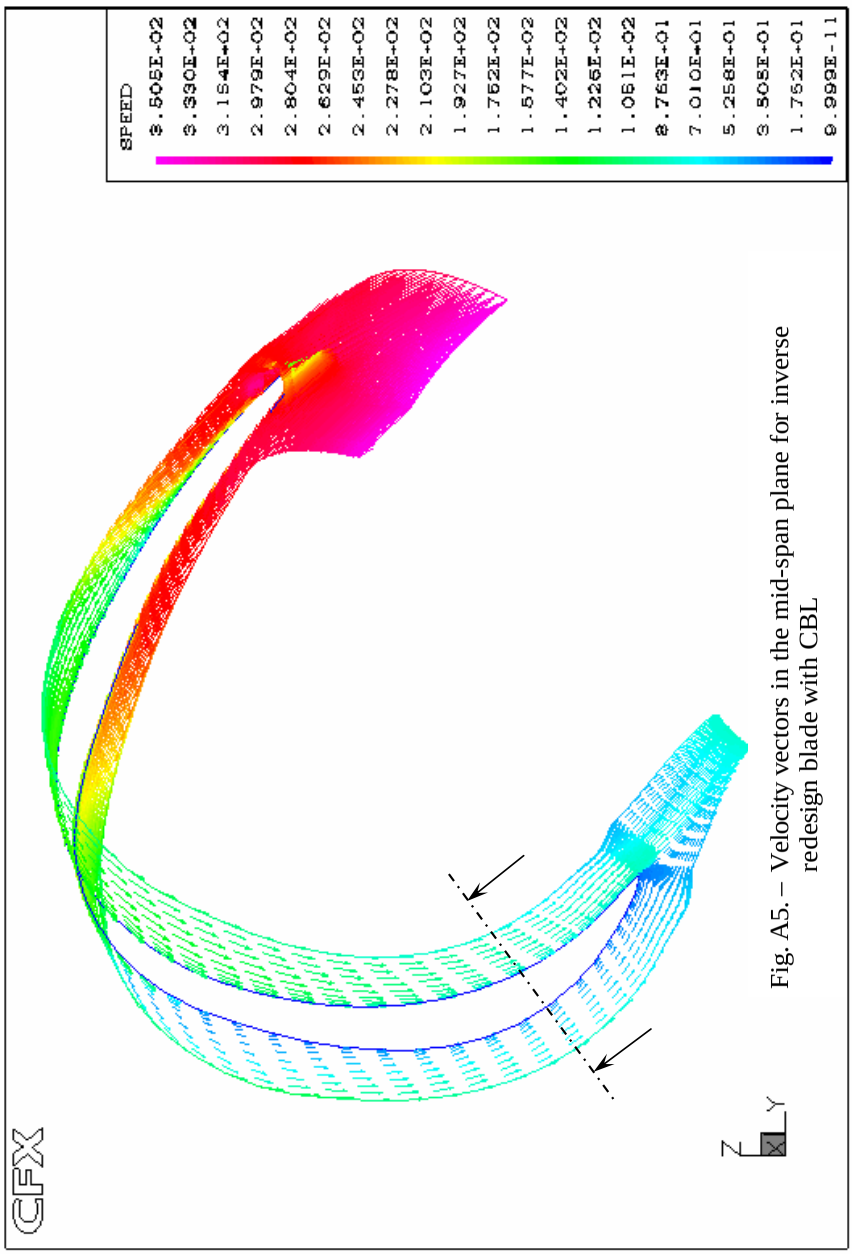

Fig. A5. – Velocity vectors in the mid-span plane for inverse redesign blade with CBL

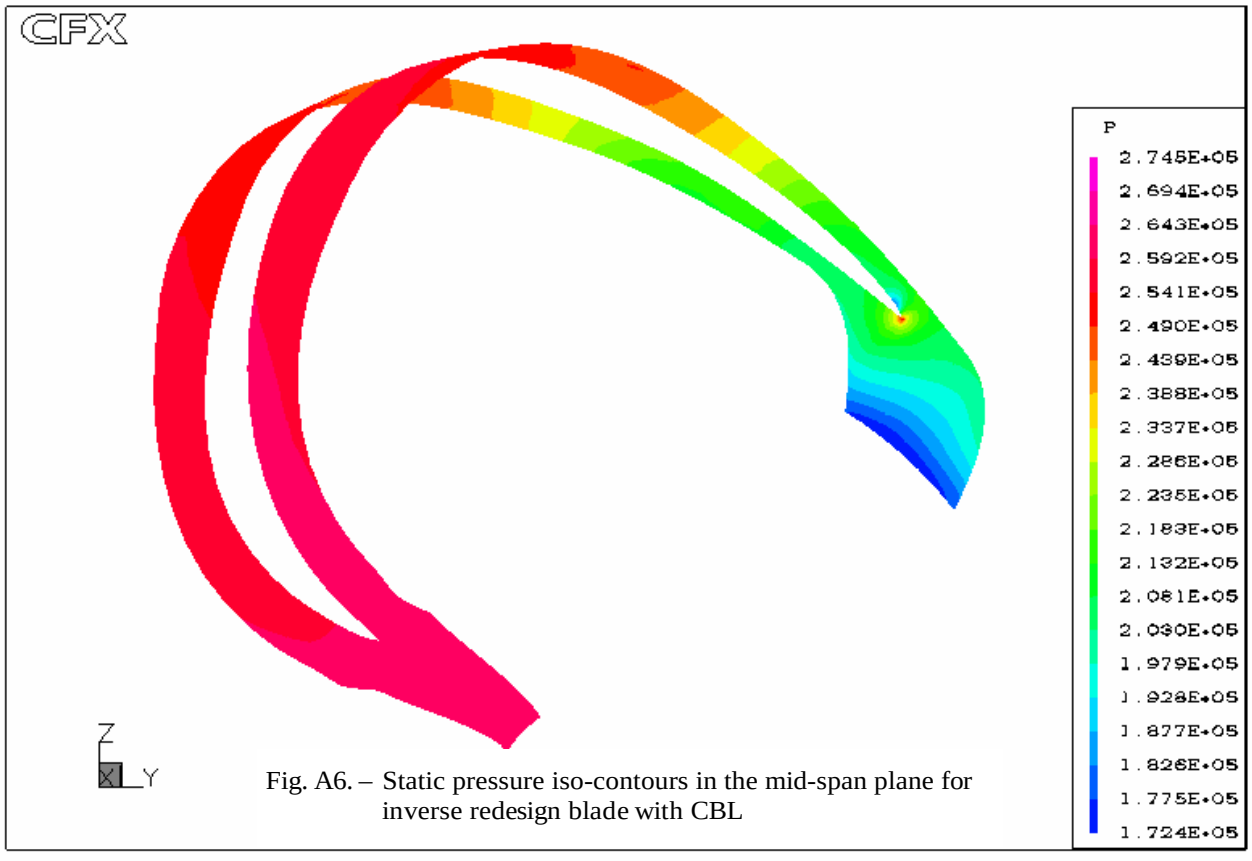

Fig. A6. – Static pressure iso-contours in the mid-span plane for inverse redesign blade with CBL

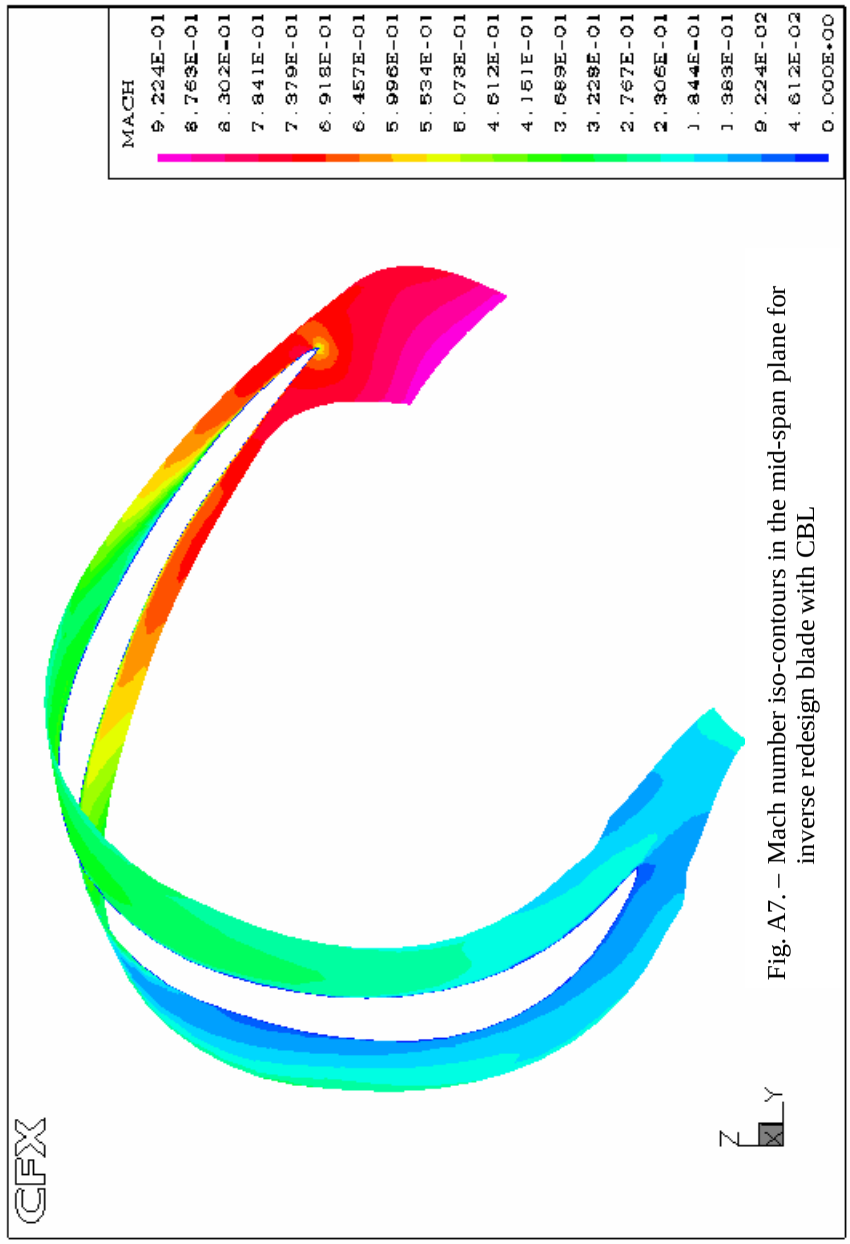

Fig. A7. – Mach number iso-contours in the mid-span plane for inverse redesign blade with CBL

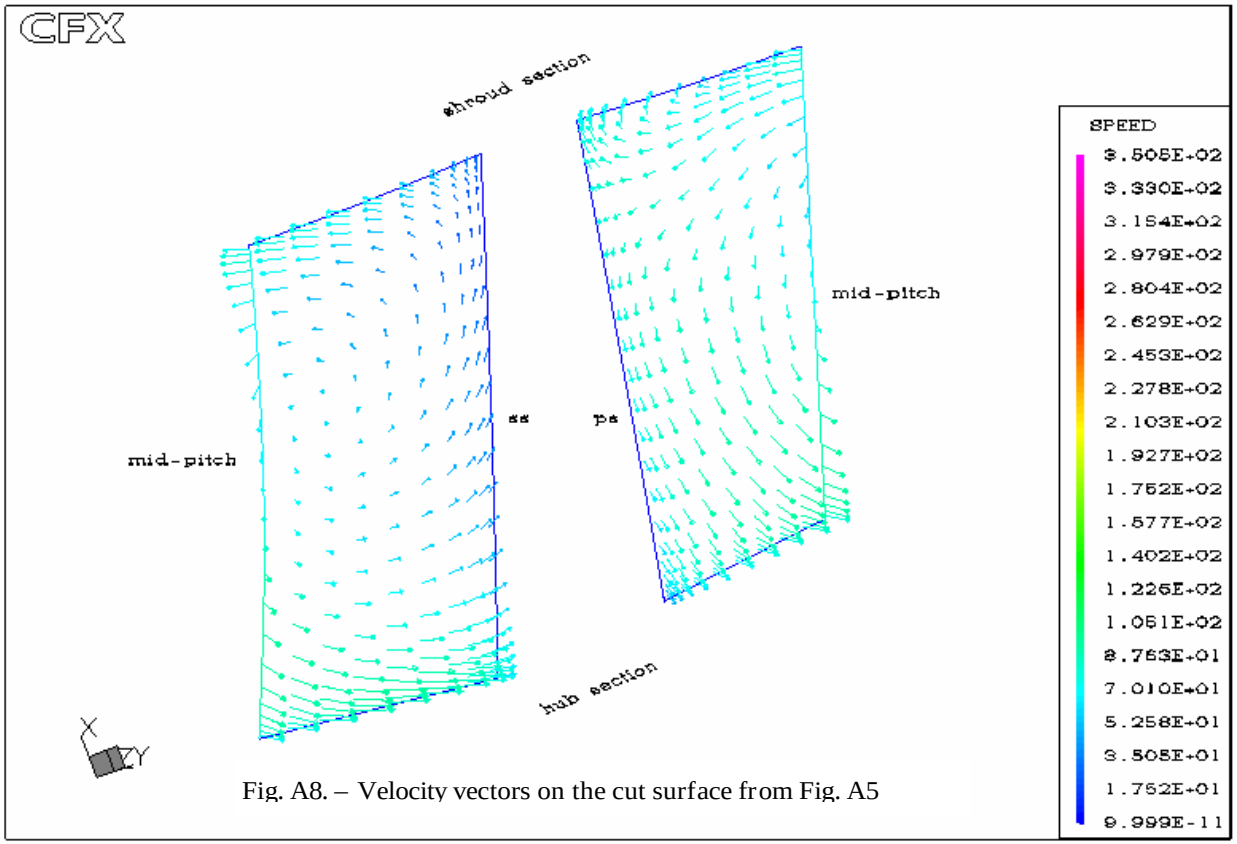

Fig. A8. – Velocity vectors on the cut surface from Fig. A5

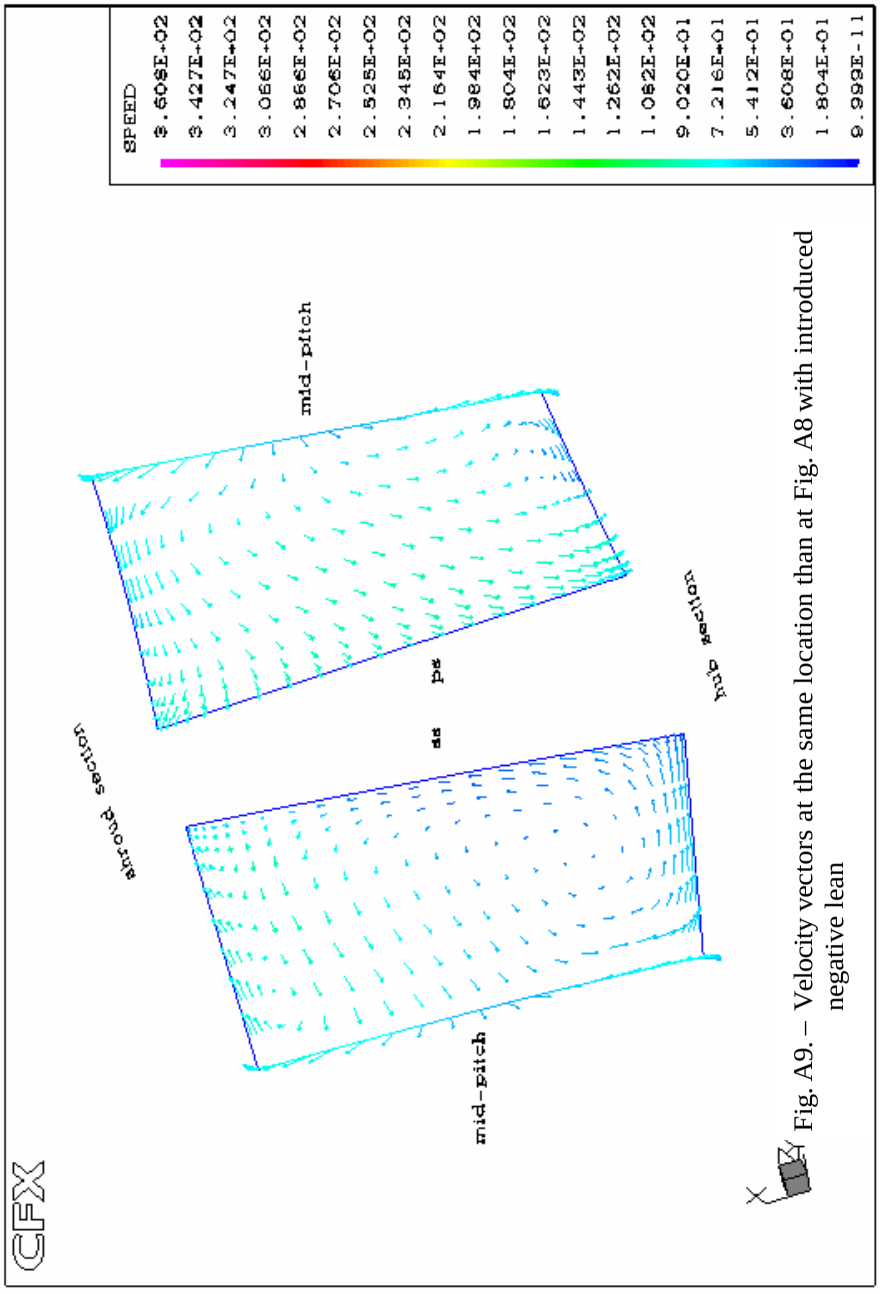

Fig. A9. – Velocity vectors at the same location than at Fig. A8 with introduced negative lean

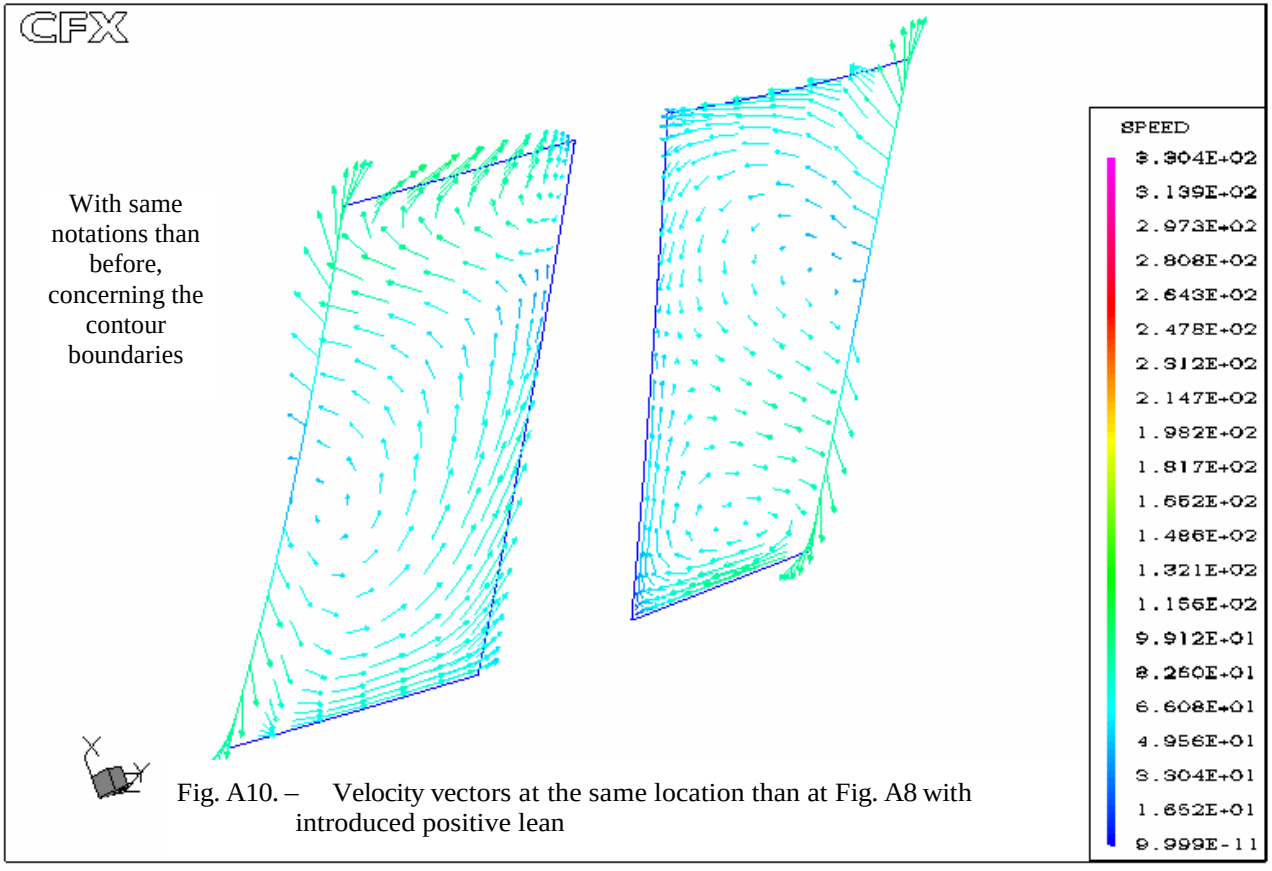

Fig. A10. – Velocity vectors at the same location than at Fig. A8 with introduced positive lean

References

[1] ROTHSTEIN, E., Experimentelle und Theoretische Untersuchung der Stroemungsvorgaenge in Rueckfuehrkanalen von Radialverdichterstufen. *Thesis*, Aachen, Germany, 1984.

[2] GAYLORD, O. E., Crossover Systems between the Stages of Centrifugal Compressors, *Journal of Basic Engineering*, March 1960.

[3] DEMEULENAERE, A., Conception et développement d'une méthode inverse pour la gmeration d'aubes de turbomachines, *Ph.D Thesis* 1997, VKI.

[4] DEMEULENAERE, A. – VAN DEN BRAEMBUSSCHE, R., Three-dimensional Inverse Method for Turbomachinery Blading Design, *ASME Journal of Turbomachinery*, **120** (1998).

[5] LEONARD,O. – VAN DEN BRAEMBUSSCHE, R., Design Method for Subsonic and Transonic Cascades with Prescribed Mach Number Distribution, *ASME Journal of Turbomachinery* **114** (1992).

[6] LEONARD, O. – VAN DEN BRAEMBUSSCHE, R., A New Compressor and Turbine Blade Design Method Based on Three-dimensional Euler Computations with Moving Boundaries, *Inverse Problems in Engineering*, **7** (1999), pp. 235–266.

[7] LEONARD, O., Inverse Methods for Airfoil Design for Aeronautical and Turbomachinery Applications, *AGARD: Report* No. 780.

[8] CALLOT, S., Inverse Blade Design by Means of a Navier–Stokes Solver, *VKI Diploma Course Project Report* 1998–04.

[9] ANTOLIN, J., Optimization of Inlet Guide Blade, *VKI Diploma Course Project Report* 1999–01.

[10] THYGESEN, R., Optimization of Return Channel Blades for Radial Compressors, *VKI Diploma Course Project Report* 2000–21.

[11] VAN DEN BRAEMBUSSCHE, R. – DEMEULENAERE, A. – BORGES, J., Inverse Design of Radial Flow Impellers with Prescribed Velocity at Hub and Shroud, *AGARD paper*, *AGARD Conference Proceedings* 537.

[12] VAN DEN BRAEMBUSSCHE, R. A., The Centrifugal Compressor Off-Design Analysis Program 'CCOD' *VKI Course Notes* 1995-06/B, July 1999.

[13] VAN DEN BRAEMBUSSCHE, R. A., Inverse Design Methods for Axial and Radial Turbomachines, *VKI Course Notes* 1994-35, May 1994.

[14] VERESS, Á., Inverse Design on Return Flow Channel for Multistage Radial Compressor, *VKI Diploma Course Project Report* 2001-27, June 2001.